IEEE Photonics Journal
An IEEE Photonics Society Publication

Open Access

Wideband and High-Resolution Measurement of Magnitude-Frequency Response for Optical Filters Based on Fixed-Low-Frequency Heterodyne Detection

Volume 9, Number 2, April 2017

Xinhai Zou
Shangjian Zhang, *Member, IEEE*
Heng Wang
Zhiyao Zhang
Jinjin Li
Yali Zhang
Shuang Liu
Yong Liu, *Senior Member, IEEE*

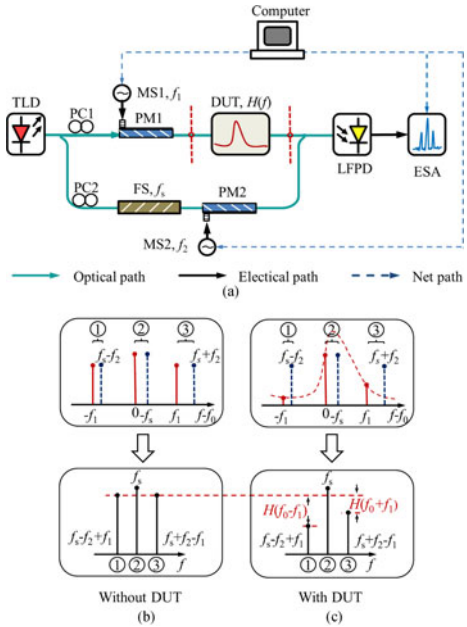

DOI: 10.1109/JPHOT.2017.2688469
1943-0655

Wideband and High-Resolution Measurement of Magnitude-Frequency Response for Optical Filters Based on Fixed-Low-Frequency Heterodyne Detection

Xinhai Zou,[1] Shangjian Zhang,[1] *Member, IEEE*, Heng Wang,[1] Zhiyao Zhang,[1] Jinjin Li,[2] Yali Zhang,[1] Shuang Liu,[1] and Yong Liu,[1] *Senior Member, IEEE*

[1]Collaboration Innovation Center of Electronic Materials and Devices, School of Optoelectronic Information, University of Electronic Science and Technology of China, Chengdu 610054, China
[2]Key Laboratory for Thin Film and Microfabrication of Ministry of Education, Department of Micro/Nano-Electronics, Shanghai Jiao Tong University, Shanghai 200240, China

DOI:10.1109/JPHOT.2017.2688469

Manuscript received January 15, 2017; revised March 21, 2017; accepted March 26, 2017. Date of publication March 28, 2017; date of current version April 12, 2017. This work was supported by the National Science Foundation of China under Grant 61377037, Grant 61421002, and Grant 61435010; in part by the Innovation Funds of Collaboration Innovation Center of Electronic Materials and Devices under Grant ICEM2015-2001; in part by the Science Foundation for Youths of Sichuan Province under Grant 2016JQ0014; and in part by the Fundamental Research Funds for the Central Universities. Corresponding author: Shangjian Zhang (e-mail: sjzhang@uestc.edu.cn).

Abstract: A high-resolution electrical method is proposed for magnitude-frequency response measurement of optical filters based on fixed-low-frequency heterodyne detection. The method consists of an acousto-optic frequency shifter and two phase modulators located in a Mach–Zehnder interferometer architecture. The modulation sidebands in the test arm pass through the optical filter under test and heterodyne with the frequency-shifted modulation sidebands in the reference arm, which allows extracting the magnitude-frequency response of the optical filter from two fixed-frequency heterodyne electrical components in the low-frequency region. In the demonstration, the magnitude-frequency response of a phase-shifted fiber Bragg grating (FBG) is experimentally extracted from low-frequency heterodyne signals fixed at 69.5 and 70.5 MHz, respectively, with hyperfine resolution up to 50 kHz and wide frequency range of 140 GHz. The proposed electrical method enables wideband magnitude-frequency response measurement for both band-pass and band-stop filters with low-frequency detection. Moreover, it features not only the immunity to modulation nonlinearity but the bidirection sweeping with doubled measurement range as well. Besides, the method only needs to receive and analyze low-frequency signals at two fixed frequencies, which largely speeds up the swept frequency measurement.

Index Terms: Microwave photonics, magnitude-frequency response, optical filters, heterodyne.

1. Introduction

Optical filters are one of key components in optical communication and optical sensing systems, in which optical filtering characteristics are crucial to signal processing and system evaluation

[1]. To date, various optical or electrical methods have been developed for measuring magnitude-frequency response of optical filters. The commonly used optical measurement approach is to use an ultra-broadband optical source, such as an amplified spontaneous emission (ASE) source or a super-continuum light source [2], [3]. This method is very efficient for wide-band measurement up to THz (tens of nm), its measurement resolution, however, is limited to be around 1.25 GHz (i.e., 0.01 nm at about 1550 nm) by the commercially available grating-based optical spectrum analyzer (OSA). Another optical measurement approach is based on the tunable diode laser spectroscopy (TDLS) scheme, in which the magnitude-frequency response is measured through wavelength sweeping of a tunable laser diode [4]. The wavelength sweeping is realized by finely adjusting the injection current, which might lead to extra intensity noise, wavelength shifting and line-width broadening, in turn degrading the measurement accuracy and stability [5]. Hence, the measurement resolution of TDLS method is reported to be about 125 MHz (1 pm @ 1550 nm) [6]. In contrast, the electrical measurement approach uses optical sideband sweeping by using either single-sideband (SSB) or double-sideband (DSB) electro-optical modulation and provides an equivalent mapping of magnitude-frequency response from the optical to electrical domain [7]–[15], which achieves a high resolution up to 78 kHz with the help of an electrical vector network analyzer [9]. The SSB-based scheme needs complex control of the optical modulation and suffers from the residual harmonic sidebands due to the modulation nonlinearity, which degrades the measurement accuracy. Furthermore, there is a trade-off between the dynamic range and the accuracy for the SSB-based method operating with small signal restriction [7] or carrier suppressing modulation [11]. The key limitation of the SSB-based method lies in that it is not efficient for measuring the band-pass response because of the degraded optical carrier in these cases [12]. In contrast, the DSB-based method achieves doubled measuring frequency range and eliminate the influence of the residual harmonic sidebands, which is based on heterodyne detection and applicable for both band-pass and band-stop optical filters [14]–[17]. Nevertheless, this method requires wide-band photodetection and signal processing, in which fast alignment of central frequency between the microwave source and the receiver is necessary at every swept frequency point.

In this paper, a wide-band and high-resolution electrical method for measuring the magnitude-frequency response of optical filters is proposed based on fixed-low-frequency heterodyne detection. Our method consists of a Mach-Zehnder heterodyne interferometer (MZHI). The modulation sidebands in the test arm of MZHI pass through the device under test (DUT) and heterodyne with the frequency-shifted modulation sidebands in the reference arm, which allows extracting the magnitude-frequency response of DUT from two fixed-frequency heterodyne components in the low-frequency region, by carefully choosing the two microwave driving frequencies. The proposed method is immunity to the undesired spurious sidebands and enables wide-band magnitude-frequency response measurement with a low-frequency heterodyne detection and processing. Moreover, it only needs to receive and analyze low-frequency signals at fixed frequencies, which largely speeds up the measurement. In the experiment, a phase-shifted fiber Bragg grating (FBG) is selected as the DUT due to the existence of narrow band window for highlighting the high-resolution measurement of the proposed method and both band-pass and band-stop windows in a representative phase-shifted FBG. The magnitude-frequency response of the phase-shifted FBG is experimentally measured based on the proposed method, where a frequency range of 140 GHz and a frequency resolution as high as 50 kHz are achieved by analyzing two heterodyne signals fixed at 70 ± 0.5 MHz. Results show that our method is applicable for measuring both band-pass and band-stop optical filters. The measured results agree well with those utilizing the optical method based on an ASE source and an OSA, which proves the consistency and accuracy of the proposed method.

2. Operation Principle

Fig. 1 presents the experimental setup and the operation principle of the proposed scheme. It consists of a MZHI, where the upper and lower paths are the test and reference arms, respectively. In the test arm, the optical carrier is firstly phase-modulated by a radio-frequency (RF) signal at

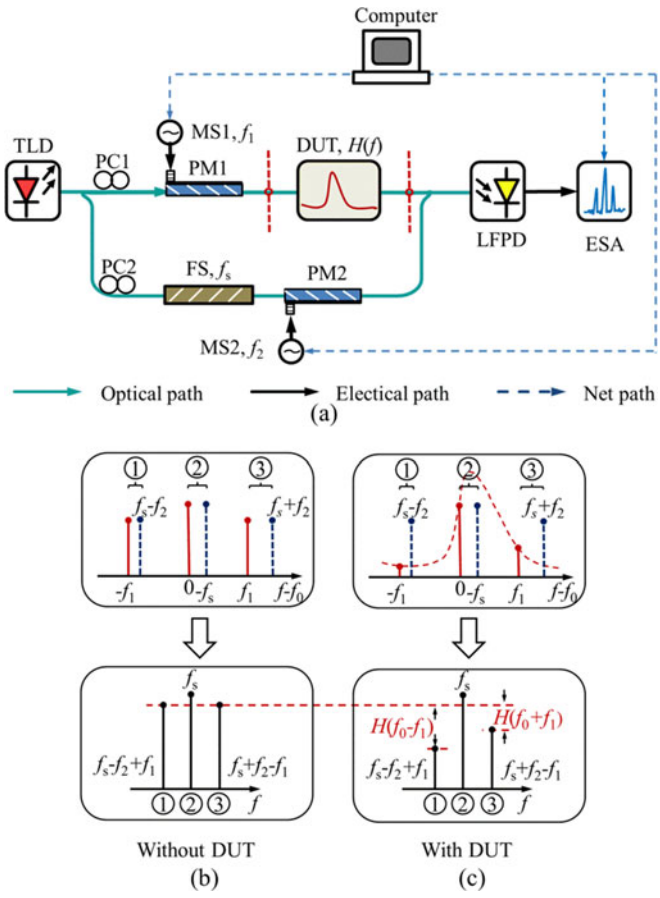

Fig. 1. Schematic diagram of the proposed scheme. (a) Experimental setup. (b) Optical spectrum (upper) and electrical spectrum (lower) without DUT. (c) Optical spectrum (upper) and electrical spectrum (lower) with DUT. TLD: tunable laser diode, PC: polarization controller, PM: phase modulator, MS: microwave source, FS: frequency shifter, DUT: device under test, LFPD: low-frequency photodetector, ESA: electrical spectrum analyzer.

the frequency of f_1, and then propagates through the optical filter under test, where the optical filter modifies the amplitude of the optical frequency components, as shown in the upper subplot of Fig. 1(c). In the reference arm, the frequency of the optical carrier is firstly shifted by f_s using an acousto-optic frequency shifter and then phase-modulated by a RF signal at the frequency of f_2, where f_2 is slightly different from f_1. The mixing process between the two arms in a low-frequency photodetector (LFPD) is called low-frequency heterodyne detection, which provides an equivalent mapping of magnitude-frequency response from optical to electrical domain as shown in Fig. 1(c). Therefore, through setting a fixed frequency difference between f_1 and f_2, the magnitude-frequency response can be obtained by simultaneously sweeping the frequencies of f_1 and f_2 and measuring the electrical power at the fixed low frequencies $f_s + f_2 - f_1$ and $f_s - f_2 + f_1$. In the following text, operation principle of the proposed scheme is mathematically introduced in detail.

In the test arm, the optical carrier at frequency f_0 is phase modulated by a single-tone RF signal at the frequency of f_1 through PM1, whose optical field can be written as

$$E_1(t) = A_1 e^{j(2\pi f_0 t + m_1 \sin 2\pi f_1 t)} = A_1 \sum_{p=-\infty}^{+\infty} J_p(m_1)\, e^{j2\pi(f_0 + p f_1)t} \tag{1}$$

where A_1 is the amplitude of the optical carrier. $J_p(.)$ is the pth-order Bessel function of the first kind. m_1 is the modulation index corresponding to the RF frequency of f_1. The optical field after the DUT is given by

$$E_1{}'(t) = A_1 \sum_{n=-\infty}^{+\infty} J_p(m_1) H(f_0 + pf_1) e^{j2\pi(f_0+pf_1)t} \tag{2}$$

where $H(f)$ is the magnitude-frequency response function of the DUT.

In the reference arm, the optical carrier is firstly frequency-shifted by f_s using FS and then modulated by another single-tone RF signal at the frequency of f_2 utilizing PM2. The optical field after PM2 can be expressed as

$$\begin{aligned} E_2(t) &= A_2 e^{j[2\pi(f_0+f_s)t + m_2 \sin 2\pi f_2 t]} \\ &= A_2 \sum_{q=-\infty}^{+\infty} J_q(m_2) e^{j2\pi(f_0+f_s+qf_2)t} \end{aligned} \tag{3}$$

where A_2 is the amplitude of the optical carrier. m_2 is the modulation index corresponding to the RF frequency of f_2.

The optical signal injected into LFPD can be expressed by the sum of the two optical signals from the two arms as

$$\begin{aligned} E(t) &= E_1{}'(t) + E_2(t) \cdot e^{j\varphi} \\ &= A_1 \sum_{p=-\infty}^{+\infty} J_p(m_1) H(f_0 + pf_1) e^{j2\pi(f_0+pf_1)t} \\ &+ A_2 \sum_{q=-\infty}^{+\infty} J_q(m_2) e^{j[2\pi(f_0+f_s+qf_2)t+\varphi]} \end{aligned} \tag{4}$$

where φ denotes the phase difference between the two arms and the phase shift of the optical coupler. The output photocurrent of LFPD can be calculated by

$$\begin{aligned} i_R &= E(t) E(t)^* \\ &= A_2^2 + 2A_1^2 \sum_p \sum_{p'=-\infty}^{+\infty} J_p(m_1) J_{p'}(m_1) H(f_0 + pf_1) \\ &\cdot H(f_0 + p'f_1) \cos\left[2\pi(p - p')f_1 t\right] \\ &+ 2A_1 A_2 \sum_p \sum_{q=-\infty}^{+\infty} J_p(m_1) J_q(m_2) H(f_0 + pf_1) \\ &\cdot \cos\left[2\pi(f_s + qf_2 - pf_1)t + \varphi\right] \end{aligned} \tag{5}$$

where R is the responsivity of LFPD and the function of frequency.

It can be seen from (5) that the amplitude of the frequency component $f_s + qf_2 - pf_1$ carries the magnitude-frequency response information of the DUT at the frequency of $f_0 + pf_1$, which can be written as

$$\begin{aligned} i_w(f_s + qf_2 - pf_1) &= 2A_1 A_2 J_p(m_1) J_q(m_2) H(f_0 + pf_1) \\ &\cdot R(f_s + qf_2 - pf_1). \end{aligned} \tag{6}$$

Therefore, through setting a fixed low frequency f_s, a fixed small difference Δ between f_1 and f_2, and sweeping frequencies f_1 and f_2 simultaneously, the magnitude-frequency response of the DUT can be obtained by analyzing the fixed-low-frequency heterodyne signals at $f_s \pm \Delta$ (i.e.,

p = 1, q = 1; p = −1, q = −1). Due to the heterodyning with undegraded reference optical sidebands, the considerable amplitude of heterodyne signals can be guaranteed with enough signal-to-noise ratio (SNR) for measuring both band-pass and band-stop magnitude-frequency responses with the proposed method.

It should be pointed out that the heterodyne signal at the frequency of $f_s + qf_2 - pf_1$ contains the response of the PMs, the DUT and the LFPD simultaneously as shown in (6). Although the heterodyne signal is measured at fixed-low-frequency, the magnitude-frequency response of the PMs indeed has a great influence on the measurement accuracy because of the large sweeping range of f_1 and f_2. In order to eliminate the impact from other devices, the calibration is performed by bypassing the DUT as

$$i_{wo}(f_s + qf_2 - pf_1) = 2A_1A_2J_p(m_1)J_q(m_2) \cdot R(f_s + qf_2 - pf_1). \quad (7)$$

According to (6) and (7), the accurate magnitude-frequency response of the DUT at frequencies of $f_0 \pm f_1$ can be calculated by

$$H(f_0 \pm f_1) = \frac{i_w[f_s \pm (f_2 - f_1)]}{i_{wo}[f_s \pm (f_2 - f_1)]}. \quad (8)$$

The advantages of the proposed scheme can be summarized as follows. First, the wide-band magnitude-frequency response can be accurately obtained by merely measuring the fixed-low-frequency heterodyne signals at $f_s \pm (f_2 - f_1)$, which only needs a low-frequency photodetection and signal processing unit and enables an improved SNR of the heterodyne frequency components due to the better performance of microwave cables, LFPD and ESA when operated in low-frequency region. Second, it only needs to receive and analyze low-frequency signals at fixed frequencies, which largely speeds up the swept frequency measurement. Thirdly, the measurement is insensitive to the power imbalance and the phase difference of the two arms thanks to the heterodyne mode instead of the interferometer mode. Furthermore, there is not small-signal assumption in the derivation from (1) to (5). As can be also seen from (8), the measurement of magnitude-frequency response is insensitive to the microwave driving powers at f_1 and f_2, indicating that our method works without small-signal restriction. Last but not the least, the RF signal at the frequency of f_1 can be used to measure the magnitude-frequency response at frequencies of $f_0 + f_1$ and $f_0 - f_1$, so the proposed method enables a doubled measuring frequency range compared to the conventional SSB-based electrical measurement method. To further extend the measuring frequency range, a series of optical carriers with a frequency offset Δf_0 can be generated by TLD and used to measure the magnitude-frequency response of the DUT in various wavelength channels. Therefore, the magnitude-frequency response of the DUT in the range of $(n-1)\Delta f_0 + 2\Delta f_1$ can be measured, where n is the number of the used optical carriers and Δf_1 is the sweeping frequency range of MS1. Through setting a frequency relationship of $\Delta f_1 < \Delta f_0 < 2\Delta f_1$, the magnitude-frequency responses of the adjacent channels can be precisely stitched to enhance the measuring frequency range, where the overlapped frequency regions can be used to calibrate the adjacent channels.

3. Experiment and Discussion

In the experiment, the optical carrier comes from a narrow-linewidth TLD whose central wavelength and output power are set to be 1550.125 nm and 11.54 dBm, respectively. In the test arm, the optical carrier is sent to a z-cut $LiNbO_3$ phase modulator (PM1, COVEGA 10027) via a polarization controller (PC) and modulated by a RF signal at the frequency of f_1 from a microwave source (MS1, R&S SMA 100A). A phase-shifted FBG is employed as the DUT, which has a narrow transmission peak in its reflection spectrum. In the experiment, the transmission spectrum of the phase-shifted FBG is measured. In the reference arm, the optical carrier is firstly frequency-shifted by 70 MHz utilizing an acousto-optic frequency shifter (FS, CETC F-FSG70), and then modulated by another RF signal at the frequency of f_2 from a microwave source (MS2, R&S SMA 100A) using a phase

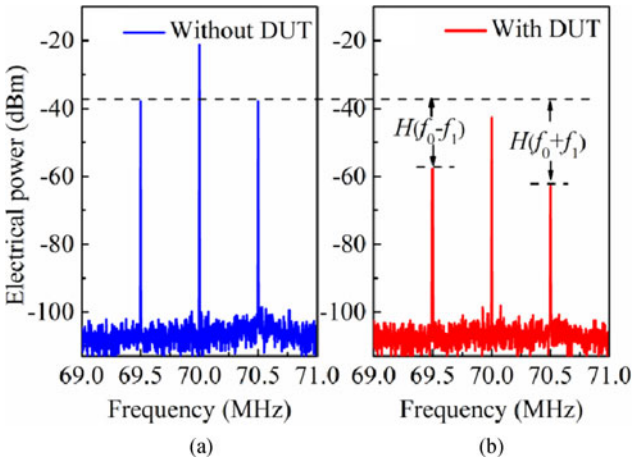

Fig. 2. Measured electrical spectrum in the case of $f_1 = 10$ GHz (a) without DUT and (b) with DUT.

modulator (PM2, COVEGA 10053). The two microwave sources are controlled by a MATLAB program via NI-VISA protocols to keep a fixed frequency difference of $\Delta = f_2 - f_1 = 0.5$ MHz, and automatically sweep f_1 from 0.1 GHz to 25 GHz with a step of 50 MHz. The combined optical signals from the two arms are detected by a LFPD with a bandwidth of 1.2 GHz. After that, the generated electrical signals are analyzed by an ESA, where the electrical power at the frequencies of 70 ± 0.5 MHz is automatically recorded by a computer.

Fig. 2(a) and (b) show the electrical spectrum without and with DUT in the case of $f_1 = 10$ GHz, respectively, where the resolution bandwidth (RBW) of the ESA is set to be 10 kHz. For demonstration, the electrical power at the frequency of $f_s + \Delta = 70.5$ MHz is measured to be -37.84 dBm and -64.21 dBm in Fig. 2(a) and (b), respectively. Based on (8), the magnitude-frequency response $H(f_0 + f_1)$ of the DUT is calculated to be -26.37 dB. Similarly, $H(f_0 - f_1)$ is determined to be -19.89 dB. Therefore, the magnitude-frequency response at two frequencies symmetric to f_0 can be measured through setting a certain value of f_1. In this case, the sweeping frequency range of f_1 in the proposed scheme can be reduced by half compared with that in the SSB-based electrical measurement method. Hence, the measurement range for a certain central frequency of f_0 is 50 GHz in our experimental setup.

The measurement can be easily operated at other frequencies of f_1 by simply setting the frequency relationship of $f_2 = f_1 + 0.0005$ GHz, as shown in Fig. 3. For each operation frequency f_1, the magnitude responses $H(f_0 \pm f_1)$ can be achieved by the same components $f_s \pm \Delta$, which is much convenient for the data collection at the fixed frequency components from the ESA and largely speeds up the swept frequency measurement. As the frequency components $f_s \pm \Delta$ are small enough to be measured with a LFPD, which the fixed-low-frequency heterodyne detection measurement is realized. To further improve the measurement efficiency and reduce the man-made error, an automatic swept measurement is involved. The MSs and ESA are connected and controlled by a computer through a GPIB data bus, with which the frequencies f_1 and f_2 are set, and the spectrum data from ESA is acquired by a MATLAB program via NI-VISA protocols.

Fig. 4 exhibits the magnitude-frequency response of the DUT in a frequency range of 140 GHz, where the blue solid line and the open circles represent the measured results using the proposed electrical method and the optical method based on an ASE source together with an OSA, respectively. The measurement range using the proposed method is limited by the sweeping frequency range of the MSs and the bandwidth of the PMs employed in our experiment setup. To further extend the measurement range, three consecutive wavelength channels are used to reconstruct the magnitude-frequency response of the DUT. A complete magnitude-frequency response of the DUT is presented by stitching the responses in the adjacent channels. Since the optical carriers of the

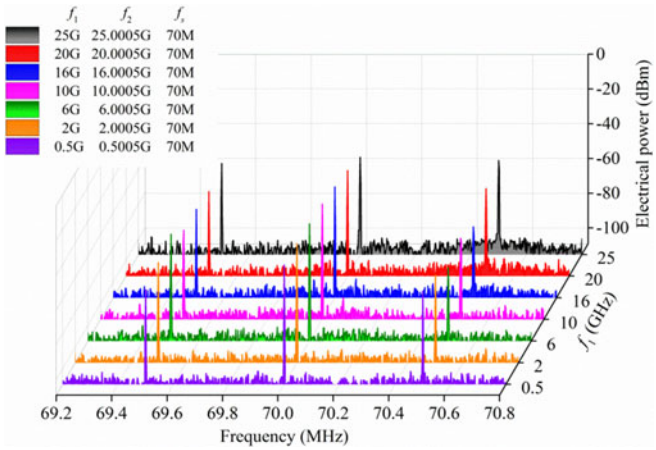

Fig. 3. Measured electrical spectrum of the heterodyne signals at the frequencies of $f_2 - f_1 - f_s$, f_s, and $f_2 - f_1 + f_s$ in cases of different modulation frequencies f_1 and f_2 with DUT.

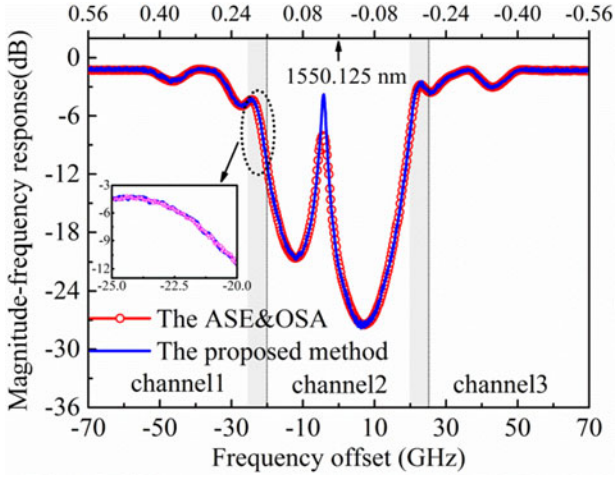

Fig. 4. Magnitude-frequency response of a phase-shifted fiber Bragg grating measured in the range of 140 GHz. (Inset) Overlapped frequency region between channel 1 and channel 2.

adjacent wavelength channels are set with a fixed frequency offset of 45 GHz and the measurement range of a single channel is 50 GHz, there is an overlapped frequency region of 5 GHz between the neighboring channels. It can be found in the inset of Fig. 4 that the magnitude-frequency responses of the adjacent channels fit well with each other in the superimposed frequency region. In addition, the measured magnitude-frequency responses employing both methods are consistent with each other except for the transmission peak in the reflection spectrum as shown in Fig. 4. The disagreement of the measurement results around the transmission peak is attributed to the different measurement resolution of the two methods, which are 50 MHz for the proposed method and 2 GHz for the method based on an ASE source and an OSA, respectively. Therefore, the proposed method can be used to accurately measure the magnitude-frequency response of an optical filter with a high-resolution. Moreover, both band-pass and band-stop magnitude-frequency responses can be measured, as can be seen from Fig. 4.

Fig. 5 presents the detail measurement of the transmission peak in a frequency range of 1 GHz with sweeping frequency steps of 50 MHz, 10 MHz, 1 MHz, and 50 kHz, respectively. As can be seen from Fig. 5, the four results agree well with each other, implying a hyperfine resolution performance

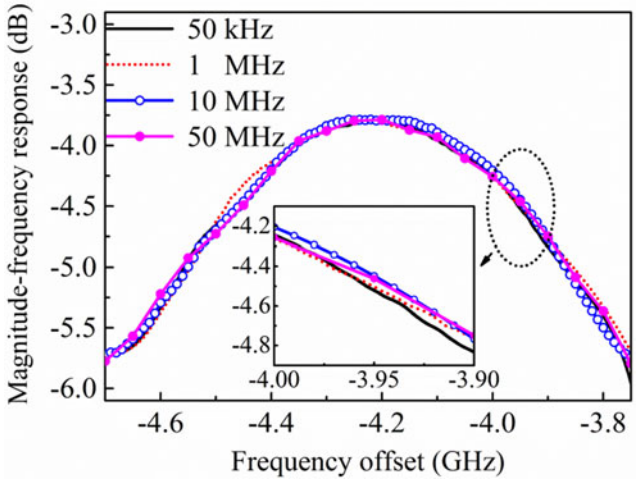

Fig. 5. Detail measurement of the transmission peak in a frequency range of 1 GHz with various sweeping frequency steps. (Inset) Zoom-in at certain range.

of the proposed method. The measurement resolution can be further improved through reducing the sweeping frequency step of f_1 and f_2, where the minimum value depends on both the RBW of ESA and the coherent status of optical signals from the two arms. In the worst incoherent case, the peak power of the heterodyne frequency components is proportional to arctan(B/δf) for the optical carrier with a Lorentz-shape spectrum, where B is the RBW of ESA and δf is the line-width of the heterodyne signal (twice of the TLD line-width) [18], [19]. In order to accurately capture the peak value of the heterodyne frequency components in the ESA, the relationship of $B > \delta f$ should be satisfied. Therefore, the measurement resolution is determined by the line-width of the TLD if the optical signals from the two arms are incoherent. In our experiment, the heterodyne frequency components exhibit delta functions in the electrical spectrum measured with a 10 kHz-resolution bandwidth as shown in Fig. 2, implying that the optical signals from the test and the reference arms are coherent. Therefore, the measurement resolution in the experiment is expected to reach 10 kHz level by further reducing the sweeping frequency step.

The amplitude measurement uncertainty of the proposed method can be written as

$$\frac{\delta H\ (f_0 \pm f_1)}{H\ (f_0 \pm f_1)} = \frac{\delta i_w\ [f_s \pm (f_2 - f_1)]}{i_w\ [f_s \pm (f_2 - f_1)]} - \frac{\delta i_{wo}\ [f_s \pm (f_2 - f_1)]}{i_{wo}\ [f_s \pm (f_2 - f_1)]} \tag{9}$$

which is derived from the total derivative of (8). $\delta H\,(f_0 \pm f_1)$ are the measurement errors of the magnitude-frequency response at the frequencies of $f_0 \pm f_1$. $\delta i_w[f_s \pm (f_2 - f_1)]$ and $\delta i_{wo}[f_s \pm (f_2 - f_1)]$ are the measurement errors of the photocurrent at the frequencies of $f_s \pm (f_2 - f_1)$ with and without DUT, respectively [20]–[22]. The uncertainty of the measured electrical power is smaller than 0.1 dB according to the specification of ESA. Therefore, the amplitude measurement uncertainty in the experiment is less than 0.2 dB, indicating that a total relative error of less than 2.33% might be delivered to the measured magnitude-frequency response in the worst case.

4. Conclusion

In summary, a novel electrical method for measuring the magnitude-frequency response of optical filters is proposed based on fixed-low-frequency heterodyne detection. The performance of the proposed method is experimentally demonstrated through measuring the magnitude-frequency response of a phase-shifted fiber Bragg grating, where a frequency range of 140 GHz and a measurement resolution as high as 50 kHz are achieved through analyzing the heterodyne electrical signals at the fixed frequencies of 70 ± 0.5 MHz. The proposed method can be used to measure

both band-pass and band-stop magnitude-frequency responses. Compared with the optical measurement approach, the proposed electrical method achieves very high-resolution up to 50 kHz. Unlike the competing DSB-based electrical method, our method enables the wide-band and high-resolution measurement for optical filters with low-frequency photodetection and signal processing. Furthermore, the proposed method works without any small-signal assumption, and it is applicable for different driving levels and operating wavelengths as long as the required frequency relationship is satisfied in the meantime, the measurement is insensitive to the power imbalance and the phase difference of the two arms due to the employment of the heterodyne mode. The measurement range can be further extended through stitching more wavelength channels, and the measurement resolution can be improved up to 10 kHz level thanks to the nature of full coherence of the proposed frequency-shifted heterodyne. Therefore, it is favorable for measuring the magnitude-frequency response of optical filters with wide frequency range and high frequency resolution.

References

[1] C. Jin *et al.*, "High-resolution optical spectrum characterization using optical channel estimation and spectrum stitching technique," *Opt. Lett.*, vol. 38, no. 13, pp. 2314–2316, Jul. 2013.

[2] G. A. Cranch and G. M. H. Flockhart, "Tools for synthesising and characterising Bragg grating structures in optical fibres and waveguides," *J. Mod. Opt.*, vol. 59, no. 6, pp. 493–526, Mar. 2012.

[3] B. Szafraniec *et al.*, "Swept coherent optical spectrum analysis, instrumentation and measurement," *IEEE Trans. Instrum. Meas.*, vol. 53, no. 1, pp. 203–215, Feb. 2004.

[4] G. D. VanWiggeren, A. R. Motamedi, and D. M. Barley, "Single-scan interferometric component analyzer," *IEEE Photon. Technol. Lett.*, vol. 15, no. 2, pp. 263–265, Feb. 2003.

[5] N. Nunoya, H. Ishii, and R. Iga, "High-speed tunable distributed amplification distributed feedback (TDA-DFB) lasers," *NTT Tech. Rev.*, vol. 10, no. 12, pp. 1–7, Dec. 2012.

[6] Y. Bao *et al.*, "A digitally generated ultrafine optical frequency comb for spectral measurements with 0.01-pm resolution and 0.7-μs response time," *Light—Sci. Appl.*, vol. 4, no. 6, Jun. 2015, Art. no. e300.

[7] W. Li, W. H. Sun, W. T. Wang, L. X. Wang, J. G. Liu, and N. H. Zhu, "Reduction of measurement error of optical vector network analyzer based on DPMZM," *IEEE Photon. Technol. Lett.*, vol. 26, no. 9, pp. 866–869, May 2014.

[8] M. Sagues and A. Loayssa, "Swept optical single sideband modulation for spectral measurement applications using stimulated Brillouin scattering," *Opt. Lett.*, vol. 18, no. 16, pp. 17555–17568, Aug. 2010.

[9] Z. Z. Tang, S. L. Pan, and J. P. Yao, "A high resolution optical vector network analyzer based on a wideband and wavelength-tunable optical single-sideband modulator," *Opt. Exp.*, vol. 20, no. 6, pp. 6555–6560, Mar. 2012.

[10] W. T. Wang, W. Li, J. G. Liu, W. H. Sun, W. Y. Wang, and N. H. Zhu, "Optical vector network analyzer with improved accuracy based on Brillouin-assisted optical carrier processing," *IEEE Photon. J.*, vol. 6, no. 6, Dec. 2014, Art. no. 5501310.

[11] M. Xue, S. L. Pan, and Y. J. Zhao, "Accuracy improvement of optical vector network analyzer based on single-sideband modulation," *Opt. Lett.*, vol. 39, no. 12, pp. 3595–3598, Jun. 2014.

[12] W. Li, W. T. Wang, L. X. Wang, and N. H. Zhu, "Optical vector network analyzer based on single-sideband modulation and segmental measurement," *IEEE Photon. J.*, vol. 6, no. 2, Apr. 2014, Art. no. 7901108.

[13] M. G. Wang and J. P. Yao, "Optical vector network analyzer based on unbalanced double-sideband modulation," *IEEE Photon. Technol. Lett.*, vol. 25, no. 8, pp. 753–756, Apr. 2013.

[14] T. Qing, M. Xue, M. H. Huang, and S. L. Pan, "Measurement of optical magnitude response based on double-sideband modulation," *Opt. Lett.*, vol. 39, no. 21, pp. 6174–6176, Nov. 2014.

[15] X. H. Zou *et al.*, "Self-calibrated electrical measurement of magnitude response of optical filters based on dual-frequency-shifted heterodyne," *Opt. Eng.*, vol. 55, no. 5, May 2016, Art. no. 056105.

[16] I. S. Ansari, M. M. Abdallah, M. S. Alouini, and K. A. Qaraqe, "Outage performance analysis of underlay cognitive RF and FSO wireless channels," in *Proc. Int. Opt. Wireless Commun.*, Nov. 2014, pp. 6–10.

[17] S. Sugavanam *et al.*, "Real-time high-resolution heterodyne-based measurements of spectral dynamics in fibre lasers," *Sci. Rep.*, vol. 6, Mar. 2016, Art. no. 23152.

[18] D. M. Baney and W. V. Sorin, "Broadband frequency characterization of optical receivers using intensity noise," *Hewlett Packard J.*, vol. 46, pp. 6–12, Feb. 1995.

[19] N. H. Zhu, J. M. Wen, H. S. San, H. P. Huang, L. J. Zhao, and W. Wang, "Improved optical heterodyne methods for measuring frequency responses of photodetectors," *IEEE J. Quantum Elect.*, vol. 42, no. 3, pp. 241–248, Mar. 2006.

[20] S. J. Zhang, H. Wang, X. H. Zou, Y. L. Zhang, R. G. Lu, and Y. Liu, "Calibration-free electrical spectrum analysis for microwave characterization of optical phase modulators using frequency-shifted heterodyning," *IEEE Photon. J.*, vol. 6, no. 4, Aug. 2014, Art. no. 5501008.

[21] S. J. Zhang, C. Zhang, H. Wang, X. H. Zou, Y. Liu, and J. E. Bowers, "Calibration-free measurement of high-speed Mach-Zehnder modulator based on low-frequency detection," *Opt. Lett.*, vol. 41, no. 3, pp. 460–463, Feb. 2016.

[22] S. J. Zhang *et al.*, "Optical frequency-detuned heterodyne for self-referenced measurement of photodetectors," *IEEE Photon. Technol. Lett.*, vol. 27, no. 8, pp. 785–788, Feb. 2015.